



Interfacial Phonon Transport Through Si/Ge Multilayer Film Using Monte Carlo Scheme With Spectral Transmissivity

Xin Ran¹, Yangyu Guo¹, Zhiyu Hu² and Moran Wang^{1*}

¹ Key Laboratory for Thermal Science and Power Engineering of Ministry of Education, Department of Engineering Mechanics and Center for Nano and Micro Mechanics (CNMM), Tsinghua University, Beijing, China, ² Department of Micro/Nano Electronics, Institute of NanoMicroEnergy, Shanghai Jiao Tong University, Shanghai, China

OPEN ACCESS

Edited by:

Nuo Yang,
Huazhong University of Science and
Technology, China

Reviewed by:

Ming Hu,
University of South Carolina,
United States
Qing Hao,
University of Arizona, United States
Jian Wang,
Yangzhou University, China

*Correspondence:

Moran Wang
moralwang@gmail.com

Specialty section:

This article was submitted to
Nanoenergy Technologies and
Materials,
a section of the journal
Frontiers in Energy Research

Received: 22 January 2018

Accepted: 29 March 2018

Published: 01 May 2018

Citation:

Ran X, Guo Y, Hu Z and Wang M
(2018) Interfacial Phonon Transport
Through Si/Ge Multilayer Film Using
Monte Carlo Scheme With Spectral
Transmissivity.
Front. Energy Res. 6:28.
doi: 10.3389/fenrg.2018.00028

The knowledge of interfacial phonon transport accounting for detailed phonon spectral properties is desired because of its importance for design of nanoscale energy systems. In this work, we investigate the interfacial phonon transport through Si/Ge multilayer films using an efficient Monte Carlo scheme with spectral transmissivity, which is validated for cross-plane phonon transport through both Si/Ge single-layer and Si/Ge bi-layer thin films by comparing with the discrete-ordinates solution. Different thermal boundary conductances between even the same material pair are declared at different interfaces within the multilayer system. Furthermore, the thermal boundary conductances at different interfaces show different trends with varying total system size, with the variation slope, very different as well. The results are much different from those in the bi-layer thin film or periodic superlattice. These unusual behaviors can be attributed to the combined interfacial local non-equilibrium effect and constraint effect from other interfaces.

Keywords: interfacial phonon transport, Monte Carlo method, micro- and nanoscale heat transport, multilayer film, material pair

INTRODUCTION

In the 1950s, semiconductors became to be used as thermoelectric material for energy conversion in refrigeration (Majumdar, 2004). The efficiency of thermoelectric material can be quantitatively determined by its dimensionless figure of merit, $ZT = S^2 \sigma T / k$, where S is the Seebeck coefficient, σ is the electrical conductivity, T is the absolute temperature, and k is the thermal conductivity (Jeng et al., 2008). To achieve a highly efficient thermoelectric device, ZT should be larger than 3, whereas for the conventional bulk materials, ZT only lies between 0.6 and 1 around room temperature (Majumdar, 2004). Recently, thermoelectrics play an appealing role toward the global energy crisis due to their direct conversion of heat to electricity in an environmentally friendly way (Wu and Wu, 2016). Therefore, there is a strong desire for the development of highly efficient thermoelectric materials. With the rapid development of nanoengineering in the past decades, people have attained significant increase of thermoelectric efficiency by nanostructuring, such as superlattices and nanocomposites (Majumdar, 2004; Kim et al., 2006; Dresselhaus et al., 2007; Jeng et al., 2008; Joshi et al., 2008; Snyder and Toberer, 2008; Hu and Poulidakos, 2012; Wu and Wu, 2016). When the size of nanostructures is smaller than the phonon mean free path (MFP) but still larger than the electron MFP, the fruitful interfaces contribute to large reduction of the thermal conductivity with negligible destruction of the electrical conductivity. In spite of the substantial

improvement of thermoelectric efficiency, a further progress remains challenging due to the elusive understanding of interfacial phonon scattering in micro and nanomaterials.

There exist several approaches in studying phonon transport across interfaces, mainly including molecular dynamics simulation (Schelling et al., 2002; Landry and McGaughey, 2009; Sun and Murthy, 2010; Liang et al., 2014), atomistic Green's function method (Li and Yang, 2012; Tian et al., 2012), phonon Boltzmann equation modeling (Majumdar, 1993; Chen, 1998; Murthy and Mathur, 2002; Jeng et al., 2008; Huang et al., 2009; Péraud and Hadjiconstantinou, 2011; Singh et al., 2011; Hua and Minnich, 2014; Hori et al., 2015; Guo and Wang, 2016; Yang and Minnich, 2017), and experimental measurements (Norris and Hopkins, 2009; Minnich et al., 2011; Hua et al., 2017). The molecular dynamics simulation and atomistic Green's function method are usually suitable for relatively small and simple structures due to their large consumption of computational resources. The experimental measurement is very difficult because of many uncertain factors from interfacial roughness, disorder, dislocations, etc. In contrast, the phonon Boltzmann equation modeling provides a more robust and feasible avenue with a clear physical picture of phonon scattering at the interface. Two categories of numerical schemes are available to solve the phonon Boltzmann equation: (i) the deterministic method [discrete-ordinates method (Majumdar, 1993; Chen, 1998), finite volume method (Murthy and Mathur, 2002), lattice Boltzmann method (Guo and Wang, 2016), etc.], (ii) the stochastic method (Monte Carlo scheme; Jeng et al., 2008; Huang et al., 2009; Péraud and Hadjiconstantinou, 2011; Hua and Minnich, 2014; Hori et al., 2015; Yang and Minnich, 2017). In comparison to the deterministic methods, Monte Carlo scheme is a better choice to simulate phonon transport within complex geometries due to its simple and intuitive boundary and interface treatment.

Hitherto, there are mainly two classical models for phonon transmission coefficient in interfacial modeling based on phonon Boltzmann equation, including the acoustic mismatch model (AMM) (Little, 1959) and the diffuse mismatch model (DMM) (Swartz and Pohl, 1989). The phonon transmission coefficient is the crucial parameter in determining the thermal boundary conductance, which is defined as the heat flux across the interface over the interfacial temperature jump (Swartz and Pohl, 1989). The AMM assumes that the phonon completely specularly transmits or reflects as acoustic waves at the interface. It works well in low temperature situation while much underestimates the thermal boundary conductance at elevated temperature due to stronger Rayleigh scattering (Majumdar, 1989; Swartz and Pohl, 1989). The DMM assumes that the phonon experiences completely diffuse scattering at the interface. Previous studies have shown that the DMM is appreciably valid around room temperature for rough and disordered interface, which are common situations in realistic applications (Swartz and Pohl, 1989; Hopkins, 2013; Kakodkar and Feser, 2017). In recent years, both the experimental measurement and microscopic calculations have uncovered the strong frequency dependence of interfacial phonon transmission coefficient (Schelling et al., 2002; Li and Yang, 2012; Hua et al., 2017). The spectral

diffuse mismatch model (SDMM) is a crude approximation yet still the most appropriate theoretical model available for describing the detailed phonon spectral feature (Duda et al., 2010; Monachon et al., 2016). The coherent and incoherent phonon scatterings have been shown to synthetically influence the heat transport in multilayer films (Simkin and Mahan, 2000; Chen et al., 2005; Luckyanova et al., 2012; Ravichandran et al., 2014; Cheaito et al., 2018). Minimum thermal conductivity has been found in superlattice at the crossover from coherent to incoherent phonon transport (Simkin and Mahan, 2000; Chen et al., 2005; Ravichandran et al., 2014). For relatively large layer thickness in the currently considered multilayer system around ordinary temperature, the phase information carried by phonons is usually lost by the diffuse scattering at the rough interface or boundary (Luckyanova et al., 2012; Ravichandran et al., 2014). Therefore, the coherent phonon scattering is negligibly weak and not taken into account in the present work.

Monte Carlo modeling of interfacial phonon transport has been widely considered in previous studies (Jeng et al., 2008; Huang et al., 2009; Péraud and Hadjiconstantinou, 2011; Hua and Minnich, 2014; Hori et al., 2015; Yang and Minnich, 2017), which yet consider either gray transmission coefficient between dissimilar materials or empirical spectral transmission coefficient between grain boundaries within single material. In the present study, we introduce the SDMM into the kinetic-type Monte Carlo scheme (Péraud and Hadjiconstantinou, 2012; Péraud et al., 2014) to study the interfacial phonon transport through Si/Ge multilayer film. The remainder of this article is organized below: the numerical and physical models are given in Section Numerical and Physical Models. The numerical method is validated in Section Validations by modeling cross-plane phonon transport through both single-layer and bi-layer thin films. The results and discussions for interfacial phonon transport through Si/Ge multilayer system are presented in section Results and Discussions. The concluding remarks are finally made in section Conclusions.

NUMERICAL AND PHYSICAL MODELS

Phonon Monte Carlo scheme is a statistical approach for solving the phonon Boltzmann equation with the counterpart direct simulation Monte Carlo (DSMC) in rarefied gas flow (Bird, 1978; Hadjiconstantinou, 2000; Wang and Li, 2003, 2004). An efficient Monte Carlo scheme is adopted to model phonon transport across the Si/Ge multilayer film in the present work, namely the kinetic-type Monte Carlo scheme (Péraud and Hadjiconstantinou, 2012; Péraud et al., 2014). This scheme solves the linearized version of the energy-based deviational phonon Boltzmann equation under small temperature difference assumption (Péraud and Hadjiconstantinou, 2011, 2012; Péraud et al., 2014):

$$\frac{\partial e^d}{\partial t} + v_g(\omega, \mathbf{p}) \cdot \nabla e^d = -\frac{e^d - (e_{loc}^{eq} - e_{T_{eq}}^{eq})}{\tau(\omega, \mathbf{p}, T)}, \quad (1)$$

where $e^d = e - e_{T_{eq}}^{eq}$ is the deviational energy distribution, with the phonon energy distribution e and equilibrium energy distribution $e_{T_{eq}}^{eq} = \hbar\omega f_0(T_{eq})$ at the referenced equilibrium temperature T_{eq} , f_0 denoting the Planck distribution; v_g and τ represent the phonon group velocity and relaxation time at the phonon angular frequency ω and local equilibrium temperature T for the phonon polarization p ; $e_{loc}^{eq} = \hbar\omega f_0(T_{loc})$ denotes the pseudo-equilibrium energy distribution at the local pseudo-equilibrium temperature T_{loc} .

The kinetic Monte Carlo scheme tracks energy packets one by one, which is much different from the traditional ensemble Monte Carlo scheme tracking all the energy packets. This scheme starts with the initialization of phonon properties (frequency, polarization, group velocity, sign, initial position, and initial time) for all the energy packets used for computation. Each energy packet will be tracked until it encounters with the isothermal boundary or the simulation time approaches to the end, during which advection and scattering occur sequentially. Two kinds of scattering events are considered: the Umklapp scattering and interface scattering. The desired macroscopic statistical information (temperature, heat flux) is finally obtained by averaging over these computational energy packets at a certain time.

The SDMM is applied to treat the interface phonon scattering neglecting inelastic scattering and polarization conversion. The frequency-dependent phonon transmission coefficient from side 1 to side 2 is dependent on the wave number as Duda et al. (2010):

$$\alpha_{12}(\omega, p) = \frac{[k_{p,2}(\omega)]^2}{[k_{p,1}(\omega)]^2 + [k_{p,2}(\omega)]^2}, \quad (2)$$

where 1 and 2 denote the labels of two dissimilar materials. The frequency-dependent phonon transmission coefficient from side 2 to side 1 is derived based on the principle of detailed balance as Duda et al. (2010):

$$\alpha_{21}(\omega, p) = \frac{[k_{p,1}(\omega)]^2}{[k_{p,1}(\omega)]^2 + [k_{p,2}(\omega)]^2}. \quad (3)$$

The present spectral DMM is slightly different from the typical frequency-dependent DMM model adopted in Singh et al. (2011), which considers the polarization conversion shown to be weak elsewhere (Duda et al., 2010). The transmitted or reflected phonons keep only the frequency and polarization but change other properties following the dispersion of material at the new side. The SDMM assumes that phonons diffusely transmit or reflect when scattering with the interface (Aksamija, 2017). Thus, the direction of group velocity of the transmitted or reflected phonon is specified based on the Lambert's cosine law (Aksamija, 2017). By tracking the energy packets one by one, we can determine which scattering time is the shortest along the trajectory of the present energy packet. If the interface scattering takes place first, then one random number is generated and compared with the interfacial phonon transmission coefficient to determine its transmission or reflection. In comparison to the Monte Carlo scheme as a kind of particle method,

the deterministic numerical method (such as discrete-ordinate method) is often inconvenient in treating complex interface due to its non-trivial spatial and angular discretization near the interface.

The one-dimensional cross-plane interfacial phonon transport across a four-layer thin film made of Si and Ge is modeled, as is shown in **Figure 1**. The thickness of each layer is the same and denoted as L_0 . The left side and the right side of the whole system are kept in contact with isothermal hot source and cold source, respectively. The dispersion relation and relaxation time expressions of Si and Ge are taken from Hopkins et al. (2011) and Singh et al. (2011), respectively. We do not consider the optical phonons due to their negligible contribution to heat transport at steady state.

VALIDATIONS

In this section, the numerical scheme in section Numerical and Physical Models is validated by modeling the cross-plane phonon transport through single-layer thin film made of Si or Ge and cross-plane interfacial phonon transport across Ge/Si bi-layer thin film as shown in **Figure 2**. The benchmark is not easy and direct mainly due to the following two reasons: (a) multiple uncertain factors (such as interfacial roughness, disorder and dislocations, etc., Hopkins, 2013) in realistic interface system make a direct comparison to experimental results almost impossible; (b) the analytical expression of thermal boundary conductance (known as the Landauer formalism; Chen, 2005) is derived based on the difference of emitted phonon temperature at the interface (Simons, 1974; Chen, 1998), which is difficult to specify in Monte Carlo scheme. Therefore, a DOM scheme incorporating the SDMM is developed and validated through predicting the Landauer's thermal boundary conductance attributed to its capability to calculate the emitted phonon temperature. Then the numerical results of cross-plane temperature distributions and effective thermal conductivity or thermal boundary conductance by the DOM scheme are used as benchmarks for the present Monte Carlo scheme.

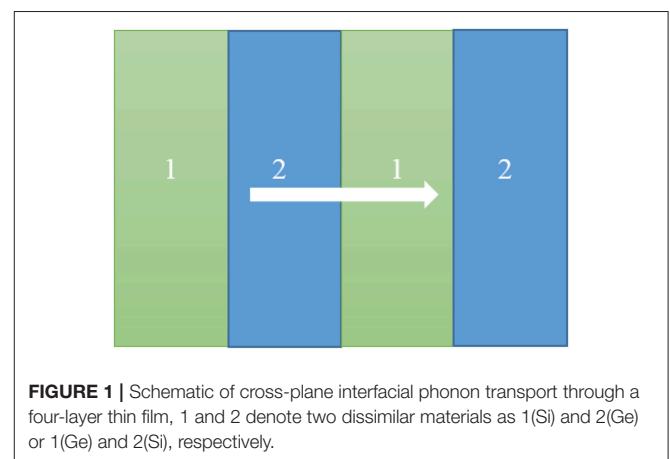
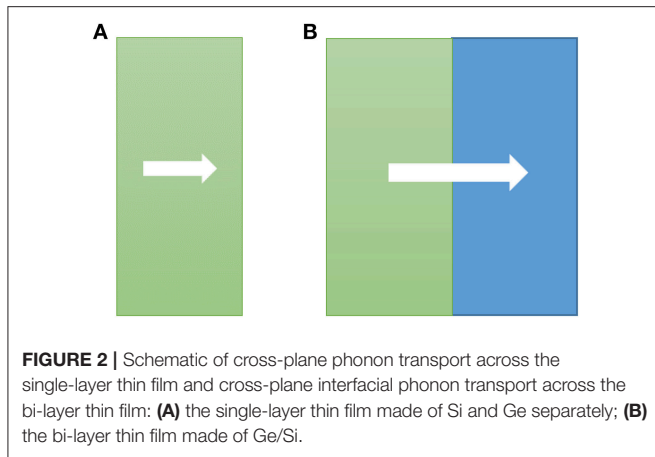


FIGURE 1 | Schematic of cross-plane interfacial phonon transport through a four-layer thin film, 1 and 2 denote two dissimilar materials as 1(Si) and 2(Ge) or 1(Ge) and 2(Si), respectively.



Cross-plane phonon transport across the single-layer thin film is firstly considered. Initially, the thin film maintains a uniform temperature as 299 K, then the temperatures of the left side (T_l) and right side (T_r) change to 301 and 299 K, respectively. Subsequently, the system evolves till it reaches the steady state. At steady state, the temperature at a spatial unit cell is computed by:

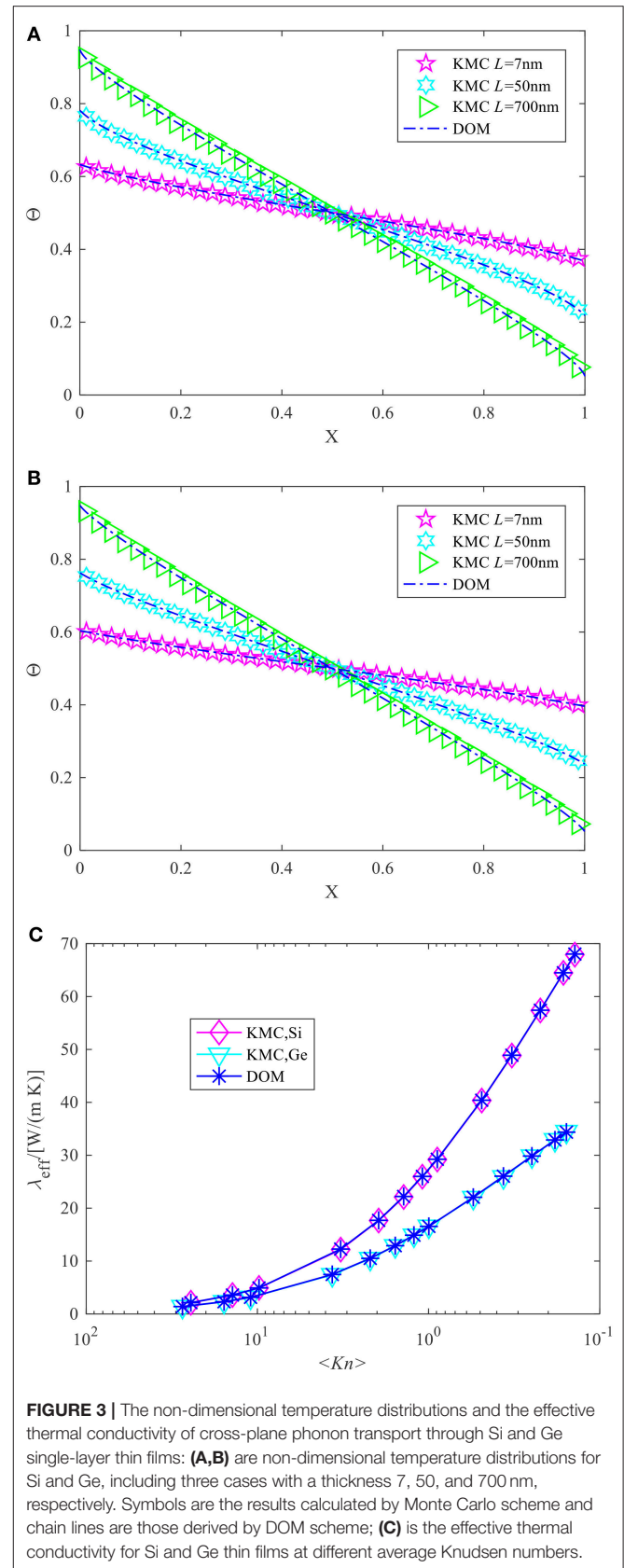
$$T = T_{eq} + \sum_i s_i \eta_{eff}^d / C_V V, \quad (4)$$

where s_i denotes the sign of tracked energy packet, η_{eff}^d being the effective deviational energy of an energy packet, C_V the volumetric heat capacity, and V is the volume of unit cell. The effective cross-plane thermal conductivity is calculated by $\lambda_{eff} = q_{ave} L / (T_l - T_r)$, where q_{ave} is the average value of heat flux along the system at steady state, and L the thickness of this thin film. To better illustrate the relation between the effective thermal conductivity and film thickness, an average Knudsen number is defined as Péraud and Hadjiconstantinou (2016):

$$\langle Kn \rangle = \frac{\bar{\Lambda}}{L}, \quad (5)$$

where the average MFP is defined as: $\bar{\Lambda} = \sum_p \int_{\omega} D \frac{de_{T_{eq}}^{eq}}{dT} v_g \tau d\omega / \sum_p \int_{\omega} D \frac{de_{T_{eq}}^{eq}}{dT} d\omega$ with the density of phonon states D . The non-dimensional temperature distributions and effective thermal conductivity for both Si and Ge thin films obtained by the present Monte Carlo scheme are compared with those by the DOM scheme in **Figure 3**, where a pretty good agreement is achieved.

The cross-plane interfacial phonon transport through the Ge/Si bi-layer thin film around room temperature is then considered. The volume ratio of the two materials keeps one for various total film thicknesses. After a period of evolutions to steady state, the temperature distributions and thermal boundary conductances are then calculated. The thermal



boundary conductance is computed based on $G = q_{ave}/\Delta T$, where ΔT is the equivalent equilibrium temperature jump across the interface. The comparison of the results calculated by Monte Carlo scheme and the DOM scheme is made in **Figure 4**, which shows a good agreement between each other. When the total thickness of thin film decreases, a stronger non-equilibrium effect at the interface gives rise to a larger temperature jump across the interface.

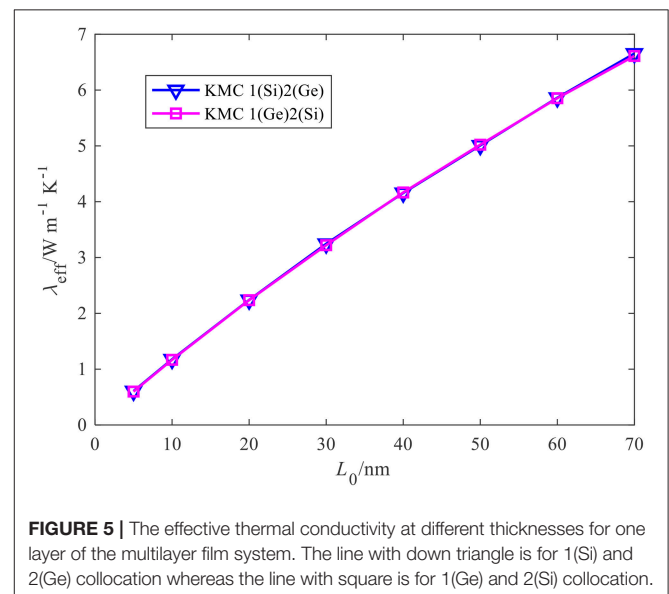
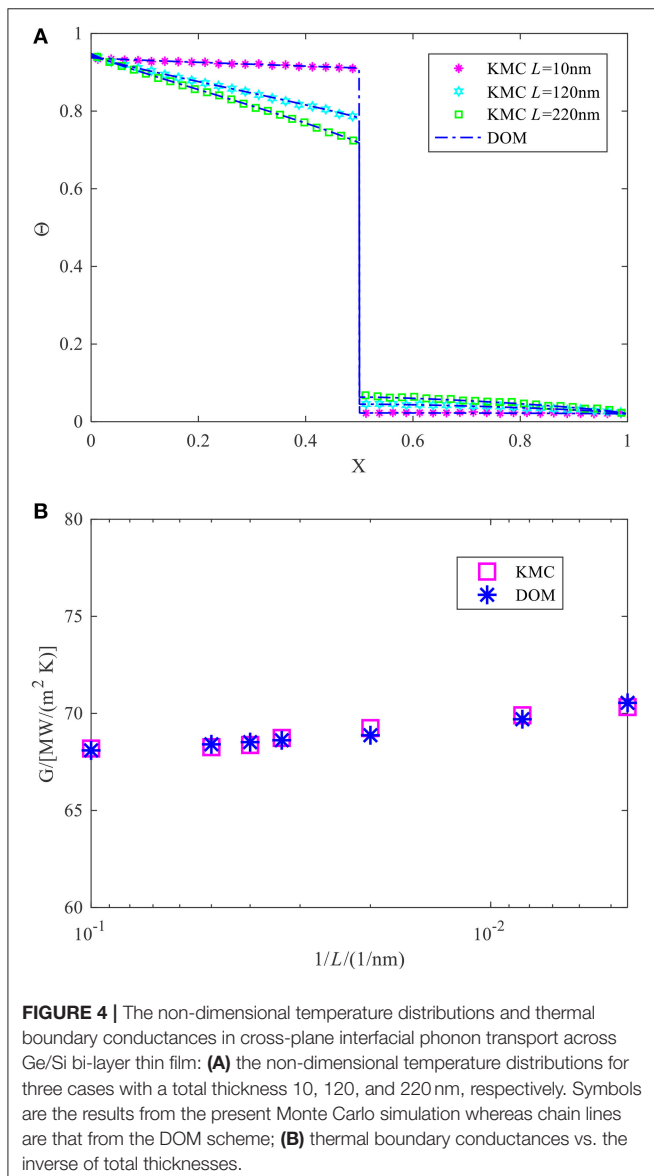
RESULTS AND DISCUSSIONS

After the present Monte Carlo scheme is validated, it is applied to study the phonon transport through a four-layer thin film as shown in **Figure 1**. The thickness L_0 of each layer is varied from 5 to 70 nm. The multilayer film system is simulated between $T_1 = 301$ K and $T_r = 299$ K, whereas the initial uniform temperature

is 299 K and the referenced temperature is $T_{eq} = 300$ K. After a sequence of evolutions, the system will reach the steady state. For 1(Si) and 2(Ge) collocation, we take the total evolving time t_{max} as 20 ns for 5–40 nm cases, 80 ns for 50 and 60 nm cases, and 120 ns for 70 nm case. The time intervals used for counting macroscopic information are 4 ps for the former two total evolving times and 6 ps for the latter one total evolving time. The total numbers of tracked energy packets are 500 million for 5–40 nm cases and 900 million for 50, 60, 70 nm cases. For 1(Ge) and 2(Si) collocation, the total evolving times t_{max} are set as 12 ns for 5–40 nm cases, and other numerical parameters are the same as those for 1(Si) and 2(Ge) collocation. Because of the fluctuations in kinetic Monte Carlo simulation, we average all the computational results from the last 30 time intervals when evaluating both the temperature and heat flux distributions.

The effective cross-plane thermal conductivity of the four-layer thin films is calculated from the uniform heat flux distribution at steady state and the exerted temperature difference based on Fourier's law: $\lambda_{eff} = 4q_{ave}L_0/(T_1 - T_r)$, which is given in **Figure 5**. The effective thermal conductivity decreases almost linearly with decreasing thickness of each layer, which is consistent with the trend shown by Chen (1998) based on a gray interface transmission coefficient in superlattice. This result shows that the linear length dependence of the effective thermal conductivity of multilayer film may be not much influenced by the phonon dispersion in the incoherent phonon transport regime. On the other hand, the thermal rectification has not been obtained when reversing the Si/Ge sequence, which may be due to a small temperature difference within the whole system.

Then the thermal boundary conductances are computed through calculating the average heat flux and the temperature jump at the interfaces. The temperature jump is extracted by fitting the temperature distributions within the four-layer system at steady state, as illustrated in **Figure 6**. The results of thermal boundary conductance are given in **Figure 7**. Four indications



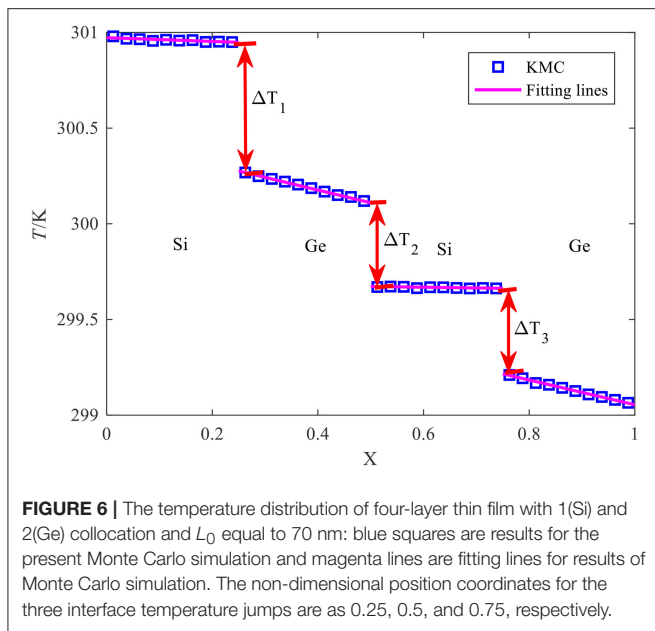


FIGURE 6 | The temperature distribution of four-layer thin film with 1(Si) and 2(Ge) collocation and L_0 equal to 70 nm: blue squares are results for the present Monte Carlo simulation and magenta lines are fitting lines for results of Monte Carlo simulation. The non-dimensional position coordinates for the three interface temperature jumps are as 0.25, 0.5, and 0.75, respectively.

are, thus, inferred: (i) the thermal boundary conductances of the interfaces that have the same relative position in the two-material collocations are almost identical. For 1(Si) and 2(Ge) collocation, its first, second, and third interfaces have nearly the same thermal boundary conductances as those of the third, second, and first interfaces of 1(Ge) and 2(Si) collocation; (ii) for a fixed thickness of one layer in multilayer film system, the thermal boundary conductances at different interfaces are different, which is similar to the conclusion in a very recent study (Gordiz and Henry, 2017); (iii) for 1(Si) and 2(Ge) system, the thermal boundary conductance of the first interface almost keeps a constant, whereas that of its second and third interfaces decrease as the thickness of each layer increases. For the other collocation, the trend is similar. In comparison, the thermal boundary conductance between material pairs within bi-layer thin film or periodic superlattice increases with increasing thickness of each layer (Balasubramanian and Puri, 2011; Jones et al., 2013). This difference is mainly attributed to different boundary or interface conditions in different interfacial structures, which directly influence the phonon scattering at boundary or interface, which will be elucidated in detail later; (iv) the decreasing slope of thermal boundary conductance at increasing thickness is different. For 1(Si) and 2(Ge) system, the decreasing rate of thermal boundary conductance at the second interface is faster than that at the third interface. For the other collocation, the trend is similar.

The indication (i) can be naturally understood. We will interpret the other three indications in terms of the material collocation 1(Si) and 2(Ge) as illustrated in **Figure 8**. For the given materials and interface, the thermal boundary conductance is dependent on the local non-equilibrium effect at the interface. Stronger local non-equilibrium at the interface results in a smaller thermal boundary conductance. Firstly, we provide a paradigm to interpret the size effect on thermal boundary

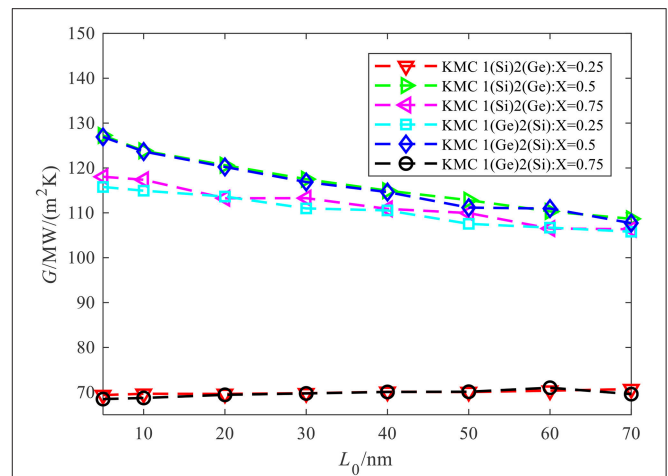


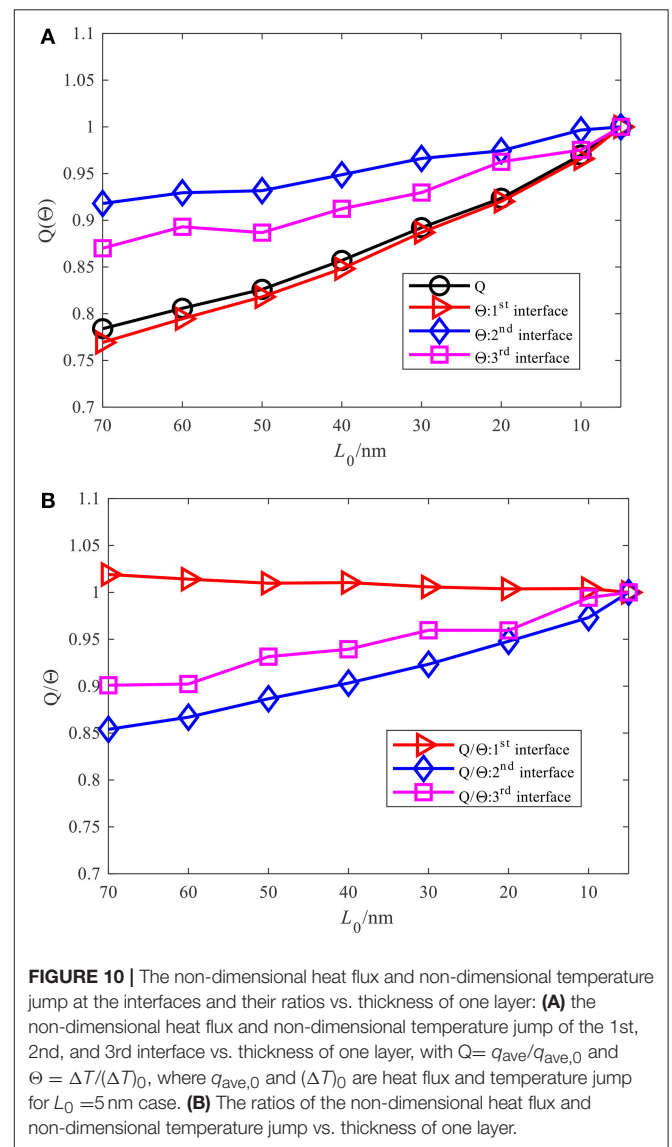
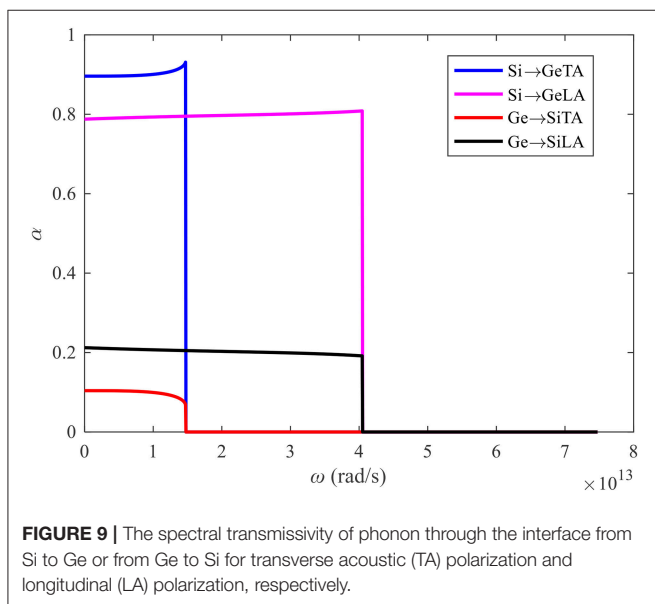
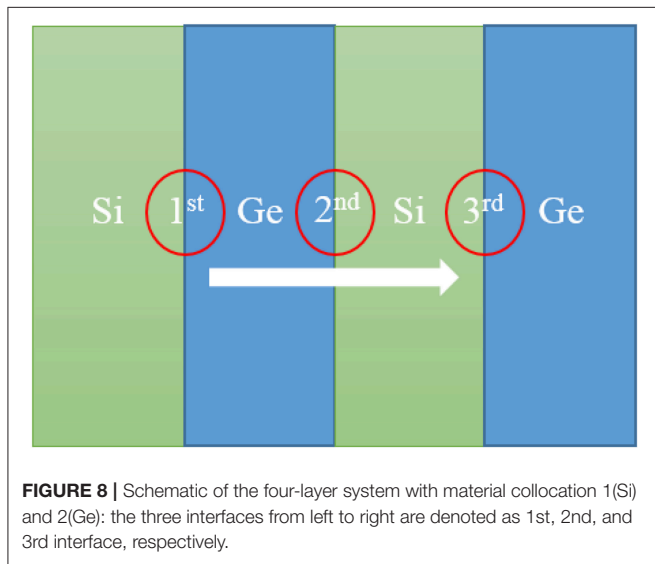
FIGURE 7 | The thermal boundary conductance of three interfaces for different material collocations vs. the thickness of one layer of the multilayer system: the red dash line with the down triangle is the result of non-dimensional position coordinates X at 0.25 for 1(Si) and 2(Ge) collocation; the green dash line with the right triangle is the result of non-dimensional position coordinates X at 0.5 for 1(Si) and 2(Ge) collocation; the magenta dash line with the left triangle is the result of non-dimensional position coordinates X at 0.75 for 1(Si) and 2(Ge) collocation; the blue-green dash line with the square is the result of non-dimensional position coordinates X at 0.25 for 1(Ge) and 2(Si) collocation; the blue dash line with the diamond is the result of non-dimensional position coordinates X at 0.5 for 1(Ge) and 2(Si) collocation; the black dash line with the circle is the result of non-dimensional position coordinates X at 0.75 for 1(Ge) and 2(Si) collocation.

conductance in bi-layer thin film in **Figure 4B**. An increase of the total thickness of bi-layer thin film is amounted to extend the boundaries with the same materials as the original film layer for each side. The contacted face between the added materials and the original film layer can be treated as two imaginary interfaces, where phonons can completely transmit without any change of properties. This will enhance the phonon-phonon interaction within the film layer and decrease the extent of non-equilibrium therein. Therefore, the local non-equilibrium effect at the interface will be reduced and the thermal boundary conductance will increase correspondingly. The indication (ii) can be explained based on a similar physical picture. The transmissivity of phonons between Si and Ge for both LA and TA polarizations based on SDMM is illustrated in **Figure 9**, which shows that the probability of phonons transmitting from Si to Ge is much larger than that in the reverse direction. For the first interface, the local non-equilibrium effect will be alleviated the least when adding the Si to Ge film layer at right side; the alleviation is improved at the third interface with the added Ge to Si film layer at the left side; the largest alleviation is achieved at the second interface where the left side and right side are added by Si and Ge, respectively. Therefore, the thermal boundary conductances of the first, third, and second interfaces increase in turn, as seen in **Figure 7**.

Finally, the indications (iii) and (iv) are explained as below. The thermal boundary conductance, $G=q_{ave}/\Delta T$, is determined by both the temperature jump at the interface and average

heat flux across system at steady state. In principle, the average heat flux will increase at decreasing system size under the given temperature difference in the present study. In contrast, the change of interface temperature jump is elusive because it is influenced by both the local non-equilibrium effect and the constraint effect from other interfaces. As the system size decreases, stronger local non-equilibrium effect tends to strengthen the interface temperature jump. However, the constraints from other interfaces will weaken the temperature jump, since the total temperature drop across the multilayer system is fixed. In other words, when the temperature jump at a specific interface is enhanced, the jump value at other interfaces will be reduced. Therefore, this kind of constraint effect from other interfaces is proportional to the local non-equilibrium

effect therein. As a result, when the system size decreases, the increase of temperature jump at the second interface is the smallest one due to both its least local non-equilibrium effect and largest constraint from the two nearby interfaces. Followed will be the third interface and first interface, respectively, as the local non-equilibrium effect at the former is smaller than that at the latter, whereas nearly the same constraint is seen from the second interface. The quantitative increasing rate of the heat flux and the interface temperature jump and their ratios with decreasing thickness are given in **Figure 10**. The non-dimensional heat flux and interface temperature jump are defined as $Q = q_{ave}/q_{ave,0}$ and $\Theta = \Delta T/(\Delta T)_0$, where $q_{ave,0}$ and $(\Delta T)_0$ are heat flux and temperature jump for $L_0 = 5$ nm case. For the second and third interfaces, the increasing rate of interface temperature jump is smaller than the increasing rate of heat flux at decreasing L_0 . Therefore, the thermal boundary conductance will even increase



at a smaller system size. For the first interface, both increasing rates are nearly the same, which results in a nearly constant thermal boundary conductance at different system sizes. This provides exactly an explanation of the indication (iii), whereas the indication (iv) can be also deduced from the preceding analysis of the relative magnitude of temperature jump increase at each interface.

CONCLUSIONS

In summary, the interfacial phonon transport through Si/Ge four-layer thin film is studied using an efficient Monte Carlo scheme with spectral transmissivity. The following points are concluded: (1) different thermal boundary conductances between the same material pair are obtained at different interfaces within the multilayer system; (2) the variation trends of the thermal boundary conductance vs. the film thickness are different at different interfaces, with the variation slope

REFERENCES

- Aksamija, Z. (2017). *Nanophononics: Thermal Generation, Transport, and Conversion at the Nanoscale*. Singapore: CRC Press.
- Balasubramanian, G., and Puri, I. K. (2011). Heat conduction across a solid-solid interface: understanding nanoscale interfacial effects on thermal resistance. *Appl. Phys. Lett.* 99:013116. doi: 10.1063/1.3607477
- Bird, G. (1978). Monte Carlo simulation of gas flows. *Ann. Rev. Fluid Mech.* 10, 11–31. doi: 10.1146/annurev.fl.10.010178.000303
- Cheaito, R., Polanco, C. A., Addamane, S., Zhang, J., Ghosh, A. W., Balakrishnan, G., et al. (2018). Interplay between total thickness and period thickness in the phonon thermal conductivity of superlattices from the nanoscale to the microscale: coherent versus incoherent phonon transport. *Phys. Rev. B.* 97:085306. doi: 10.1103/PhysRevB.97.085306
- Chen, G. (1998). Thermal conductivity and ballistic-phonon transport in the cross-plane direction of superlattices. *Phys. Rev. B.* 57:14958. doi: 10.1103/PhysRevB.57.14958
- Chen, G. (2005). *Nanoscale Energy Transport And Conversion: A Parallel Treatment Of Electrons, Molecules, Phonons, and Photons*. New York, NY: Oxford University Press.
- Chen, Y., Li, D., Lukes, J. R., Ni, Z., and Chen, M. (2005). Minimum superlattice thermal conductivity from molecular dynamics. *Phys. Rev. B.* 72:174302. doi: 10.1103/PhysRevB.72.174302
- Dresselhaus, M. S., Chen, G., Tang, M. Y., Yang, R. G., Lee, H., Wang, D. Z., et al. (2007). New directions for low-dimensional thermoelectric materials. *Adv. Mater.* 19, 1043–1053. doi: 10.1002/adma.200600527
- Duda, J. C., Hopkins, P. E., Smoyer, J. L., Bauer, M. L., English, T. S., Saltonstall, C. B., et al. (2010). On the assumption of detailed balance in prediction of diffusive transmission probability during interfacial transport. *Nanoscale Microscale Thermophys. Eng.* 14, 21–33. doi: 10.1080/15567260903530379
- Gordiz, K., and Henry, A. (2017). Phonon transport at interfaces between different phases of silicon and germanium. *J. Appl. Phys.* 121:025102. doi: 10.1063/1.4973573
- Guo, Y., and Wang, M. (2016). Lattice Boltzmann modeling of phonon transport. *J. Comput. Phys.* 315, 1–15. doi: 10.1016/j.jcp.2016.03.041
- Hadjiconstantinou, N. G. (2000). Analysis of discretization in the direct simulation Monte Carlo. *Phys. Fluids.* 12, 2634–2638. doi: 10.1063/1.1289393
- Hopkins, P. E. (2013). Thermal transport across solid interfaces with nanoscale imperfections: effects of roughness, disorder, dislocations, and bonding on thermal boundary conductance. *ISRN Mech. Eng.* 2013:682586. doi: 10.1155/2013/682586
- Hopkins, P. E., Reinke, C. M., Su, M. F., Olsson, R. H., Shaner, E. A., Leseman, Z. C., et al. (2011). Reduction in the thermal conductivity of single crystalline silicon by phononic crystal patterning. *Nano Lett.* 11, 107–112. doi: 10.1021/nl102918q
- Hori, T., Shiomi, J., and Dames, C. (2015). Effective phonon mean free path in polycrystalline nanostructures. *Appl. Phys. Lett.* 106:171901. doi: 10.1063/1.4918703
- Hu, M., and Poulidakos, D. (2012). Si/Ge superlattice nanowires with ultralow thermal conductivity. *Nano Lett.* 12, 5487–5494. doi: 10.1021/nl301971k
- Hua, C., Chen, X., Ravichandran, N. K., and Minnich, A. J. (2017). Experimental metrology to obtain thermal phonon transmission coefficients at solid interfaces. *Phys. Rev. B.* 95:205423. doi: 10.1103/PhysRevB.95.205423
- Hua, C., and Minnich, A. J. (2014). Importance of frequency-dependent grain boundary scattering in nanocrystalline silicon and silicon-germanium thermoelectrics. *Semicond. Sci. Tech.* 29:124004. doi: 10.1088/0268-1242/29/12/124004
- Huang, M. J., Tsai, T. C., Liu, L. C., Jeng, M. S. and Yang, C. C. (2009). A fast Monte-Carlo solver for phonon transport in nanostructured semiconductors. *Comput. Model. Eng. Sci.* 42, 107–130. doi: 10.3970/cmcs.2009.042.107
- Jeng, M.-S., Yang, R., Song, D., and Chen, G. (2008). Modeling the thermal conductivity and phonon transport in nanoparticle composites using monte carlo simulation. *J. Heat Transfer* 130:042410. doi: 10.1115/1.2818765
- Jones, R. E., Duda, J. C., Zhou, X. W., Kimmer, C. J., and Hopkins, P. E. (2013). Investigation of size and electronic effects on Kapitza conductance with non-equilibrium molecular dynamics. *Appl. Phys. Lett.* 102:183119. doi: 10.1063/1.4804677
- Joshi, G., Lee, H., Lan, Y., Wang, X., Zhu, G., Wang, D., et al. (2008). Enhanced thermoelectric figure-of-merit in nanostructured p-type silicon germanium bulk alloys. *Nano Lett.* 8, 4670–4674. doi: 10.1021/nl8026795
- Kakodkar, R. R., and Feser, J. P. (2017). Probing the validity of the diffuse mismatch model for phonons using atomistic simulations. *Phys. Rev. B* 95:024102. doi: 10.1103/PhysRevB.95.125434
- Kim, W., Zide, J., Gossard, A., Klenov, D., Stemmer, S., Shakouri, A., et al. (2006). Thermal conductivity reduction and thermoelectric figure of merit increase by embedding nanoparticles in crystalline semiconductors. *Phys. Rev. Lett.* 96:045901. doi: 10.1103/PhysRevLett.96.045901
- Landry, E. S., and McGaughey, A. J. H. (2009). Thermal boundary resistance predictions from molecular dynamics simulations and theoretical calculations. *Phys. Rev. B* 80:165304. doi: 10.1103/PhysRevB.80.165304
- Li, X., and Yang, R. (2012). Effect of lattice mismatch on phonon transmission and interface thermal conductance across dissimilar material interfaces. *Phys. Rev. B* 86:054305. doi: 10.1103/PhysRevB.86.054305

AUTHOR CONTRIBUTIONS

MW organized the research. XR did the MC simulations. YG modified the theoretical model. ZH participated discussions on mechanisms. XR and YG wrote the manuscript, and MW and ZH finalized it.

ACKNOWLEDGMENTS

This work is financially supported by NSF of China (No. 91634107, 51621062).

- Liang, Z., Sasikumar, K., and Keblinski, P. (2014). Thermal transport across a substrate-thin-film interface: effects of film thickness and surface roughness. *Phys. Rev. Lett.* 113:065901. doi: 10.1103/PhysRevLett.113.065901
- Little, W. (1959). The transport of heat between dissimilar solids at low temperatures. *Can. J. Phys.* 37, 334–349. doi: 10.1139/p59-037
- Luckyanova, M. N., Garg, J., Esfarjani, K., Jandl, A., Bulsara, M. T., Schmidt, A. J., et al. (2012). Coherent phonon heat conduction in superlattices. *Science* 338, 936–939. doi: 10.1126/science.1225549
- Majumdar, A. (1989). Effect of interfacial roughness on phonon radiative heat conduction. *ASME. Trans. J. Heat Transfer* 113, 797–805. doi: 10.1115/1.2911206
- Majumdar, A. (1993). Microscale heat conduction in dielectric thin films. *J. Heat Transfer* 115, 7–16. doi: 10.1115/1.2910673
- Majumdar, A. (2004). Thermoelectricity in semiconductor nanostructures. *Science* 303, 777–778. doi: 10.1126/science.1093164
- Minnich, A. J., Johnson, J., Schmidt, A., Esfarjani, K., Dresselhaus, M., Nelson, K. A., et al. (2011). Thermal conductivity spectroscopy technique to measure phonon mean free paths. *Phys. Rev. Lett.* 107:095901. doi: 10.1103/PhysRevLett.107.095901
- Monachon, C., Weber, L., and Dames, C. (2016). Thermal boundary conductance: a materials science perspective. *Ann. Rev. Mater. Res.* 46, 433–463. doi: 10.1146/annurev-matsci-070115-031719
- Murthy, J. Y., and Mathur, S. R. (2002). Computation of sub-micron thermal transport using an unstructured finite volume method. *J. Heat Transfer* 124, 1176–1181. doi: 10.1115/1.1518495
- Norris, P. M., and Hopkins, P. E. (2009). Examining interfacial diffuse phonon scattering through transient thermoreflectance measurements of thermal boundary conductance. *J. Heat Transfer* 131:043207. doi:10.1115/1.3072928
- Péraud, J.-P. M., and Hadjiconstantinou, N. G. (2011). Efficient simulation of multidimensional phonon transport using energy-based variance-reduced Monte Carlo formulations. *Phys. Rev. B* 84:205331. doi: 10.1103/PhysRevB.84.205331
- Péraud, J.-P. M., and Hadjiconstantinou, N. G. (2012). An alternative approach to efficient simulation of micro/nanoscale phonon transport. *Appl. Phys. Lett.* 101:1.4757607. doi: 10.1063/1.4757607
- Péraud, J.-P. M., and Hadjiconstantinou, N. G. (2016). Extending the range of validity of Fourier's law into the kinetic transport regime via asymptotic solution of the phonon Boltzmann transport equation. *Phys. Rev. B* 93:045424. doi: 10.1103/PhysRevB.93.045424
- Péraud, J.-P. M., Landon, C. D., and Hadjiconstantinou, N. G. (2014). Monte Carlo methods for solving the Boltzmann transport equation. *Ann. Rev. Heat Transfer* 17, 205–265. doi: 10.1615/AnnualRevHeatTransfer.2014007381
- Ravichandran, J., Yadav, A. K., Cheaito, R., Rossen, P. B., Soukiassian, A., Suresha, S. J., et al. (2014). Crossover from incoherent to coherent phonon scattering in epitaxial oxide superlattices. *Nat. Mater.* 13, 168–172. doi: 10.1038/nmat3826
- Schelling, P. K., Phillpot, S. R., and Keblinski, P. (2002). Phonon wave-packet dynamics at semiconductor interfaces by molecular-dynamics simulation. *Appl. Phys. Lett.* 80, 2484–2486. doi: 10.1063/1.1465106
- Simkin, M., and Mahan, G. (2000). Minimum thermal conductivity of superlattices. *Phys. Rev. Lett.* 84, 927–930. doi: 10.1103/PhysRevLett.84.927
- Simons, S. (1974). On the thermal contact resistance between insulators. *J. Phys. C* 7, 4048–4052. doi: 10.1088/0022-3719/7/22/009
- Singh, D., Murthy, J. Y., and Fisher, T. S. (2011). Effect of phonon dispersion on thermal conduction across Si/Ge interfaces. *J. Heat Transfer* 133:122401. doi: 10.1115/1.4004429
- Snyder, G. J., and Toberer, E. S. (2008). Complex thermoelectric materials. *Nat. Mater.* 7, 105–114. doi: 10.1038/nmat2090
- Sun, L., and Murthy, J. Y. (2010). Molecular dynamics simulation of phonon scattering at silicon/germanium interfaces. *J. Heat Transfer* 132:102403. doi: 10.1115/1.4001912
- Swartz, E. T., and Pohl, R. O. (1989). Thermal boundary resistance. *Rev. Modern Phys.* 61, 605–668. doi: 10.1103/RevModPhys.61.605
- Tian, Z., Esfarjani, K., and Chen, G. (2012). Enhancing phonon transmission across a Si/Ge interface by atomic roughness: first-principles study with the Green's function method. *Phys. Rev. B* 86:235304. doi: 10.1103/PhysRevB.86.235304
- Wang, M., and Li, Z. (2003). Nonideal gas flow and heat transfer in micro- and nanochannels using the direct simulation Monte Carlo method. *Phys. Rev. E* 68:046704. doi: 10.1103/PhysRevE.68.046704
- Wang, M., and Li, Z. (2004). Simulations for gas flows in microgeometries using the direct simulation Monte Carlo method. *Int. J. Heat Fluid Flow* 25, 975–985. doi: 10.1016/j.ijheatfluidflow.2004.02.024
- Wu, C. -W., and Wu, Y.-R. (2016). Optimization of thermoelectric properties for rough nano-ridge GaAs/AlAs superlattice structure. *AIP Adv.* 6:115201. doi: 10.1063/1.4967202
- Yang, L., and Minnich, A. J. (2017). Thermal transport in nanocrystalline Si and SiGe by ab initio based Monte Carlo simulation. *Sci. Rep.* 7:44254. doi: 10.1038/srep44254

Conflict of Interest Statement: The authors declare that the research was conducted in the absence of any commercial or financial relationships that could be construed as a potential conflict of interest.

Copyright © 2018 Ran, Guo, Hu and Wang. This is an open-access article distributed under the terms of the Creative Commons Attribution License (CC BY). The use, distribution or reproduction in other forums is permitted, provided the original author(s) and the copyright owner are credited and that the original publication in this journal is cited, in accordance with accepted academic practice. No use, distribution or reproduction is permitted which does not comply with these terms.